JOC The Journal of Organic Chemistry

Article

pubs.acs.org/joc

Photolysis of Dimethylcarbamoyl Azide in an Argon Matrix: Spectroscopic Identification of Dimethylamino Isocyanate and 1,1-Dimethyldiazene

Tibor Pasinszki,*[,†] Melinda Krebsz,[†,‡] György Tarczay,[†] and Curt Wentrup*[,§]

[†]Institute of Chemistry, Eötvös Loránd University, P.O. Box 32, H-1518 Budapest 112, Hungary

[‡]Institute for Geological and Geochemical Research, Research Centre for Astronomy and Earth Sciences, Hungarian Academy of Sciences, 45 Budaörsi street, H-1112 Budapest, Hungary

[§]School of Chemistry and Molecular Biosciences, The University of Queensland, Brisbane, Queensland 4072, Australia

Supporting Information

ABSTRACT: The UV photolysis of dimethylcarbamoyl azide has been investigated in an argon matrix at cryogenic temperatures. The products of the photolysis were identified by infrared spectroscopy supported by quantum-chemical calculations. Sequential formation of dimethylamino isocyanate (Me_2N-NCO), 1,1-dimethyldiazene ($Me_2N=N$), and ethane was established. Therefore, the major decomposition channel is identified as $Me_2NC(O)N_3 \rightarrow Me_2N-NCO \rightarrow Me_2N=N \rightarrow Me-Me$, via consecutive N_2, CO, and N_2 eliminations. Ground-state geometries, vibrational frequencies, IR intensities, and UV excitation energies of the transient dimethylamino isocyanate and 1,1-dimethyldiazene have been computed using the B3LYP and SAC-CI methods and the aug-cc-pVTZ basis set.

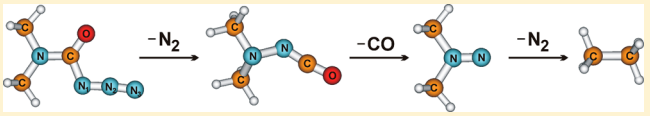

INTRODUCTION

The photo-Curtius rearrangement of carbamoyl azides is a general method to generate reactive amino isocyanates in solution for various synthetic applications.[1−3] Although amino isocyanates are widely used in addition reactions as in situ reagents, their isolation in the pure state is not possible due to their fast dimerization, even at low temperatures.[1] Direct spectroscopic identification of amino isocyanates and other reactive intermediates during the photolysis is thus challenging. Matrix isolation spectroscopy provides a unique and powerful method to study the photo-Curtius rearrangement and the photostability of amino isocyanates, as well as any other photolysis products which may contribute to the often complicated mechanism and numerous side products of solution reactions.

The photolysis of only two carbamoyl azides, the parent carbamoyl azide[4] and dimethylcarbamoyl azide,[3] have been studied to date in noble-gas matrices. IR spectroscopic evidence for the formation of amino isocyanates as primary photolysis products was provided.[3,4] It was observed that amino isocyanates were unstable upon irradiation with UV light. The parent amino isocyanate decomposed upon UV irradiation to 1,1-diazene (aminonitrene) and carbon monoxide,[5] but the decomposition of dimethylamino isocyanate was interpreted in terms of formation of an isocyanic acid−methyl isocyanide molecule pair absorbing at 2269 (HNCO) and 2141 cm^{-1} (CH_3NC).[3] Thus, apparently the decompositions of amino and dimethylamino isocyanates took different routes. In order to understand this difference, we have reinvestigated the photodecomposition of dimethylcarbamoyl azide. Here we report an experimental study on the UV photolysis of dimethylcarbamoyl azide in an Ar matrix and an investigation of its photolysis products using IR and UV spectroscopy, as well as quantum-chemical calculations.

RESULTS AND DISCUSSION

Equilibrium Structures of $(CH_3)_2N-NCO$ and $(CH_3)_2N=N$. As shown below, the principal products of photolysis of dimethylcarbamoyl azide ($(CH_3)_2N-CO-N_3$) are dimethylamino isocyanate ($(CH_3)_2N-NCO$) and 1,1-dimethyldiazene ($(CH_3)_2N=N$). Their equilibrium geometries were calculated at the B3LYP level using a large aug-cc-pVTZ basis set, and the discussion below, unless otherwise noted, is based on these results. The geometries are shown in Figures 1 and 2 and in Table S1 in the Supporting Information. Both molecules have singlet electronic ground states, which are more stable than the triplets by 162 and 83 kJ mol^{-1}, respectively ($\Delta G_{0\,K}$).

$(CH_3)_2N-NCO$ has a trans-bent NNCO frame (the NNC and NCO angles are 130.9 and 171.9°, respectively), which is typical of covalent isocyanates. The barrier to linearity is relatively high at 24 kJ mol^{-1}. The inversion barrier at the amino nitrogen atom is 27 kJ mol^{-1}. The molecular symmetry is C_1. Rotation around the N−N single bond is hindered at very low temperatures but is essentially free at room temperature (see Figure 1). The free energy difference between $(CH_3)_2N-NCO$ and the photolysis products $(CH_3)_2N=N$ + CO to be described below is only 118 kJ mol^{-1}, and the (thermal) barrier for this process is 157 kJ mol^{-1}. This is below the calculated

Received: September 11, 2013
Published: November 5, 2013

   dx.doi.org/10.1021/jo402023m | J. Org. Chem. 2013, 78, 11985−11991

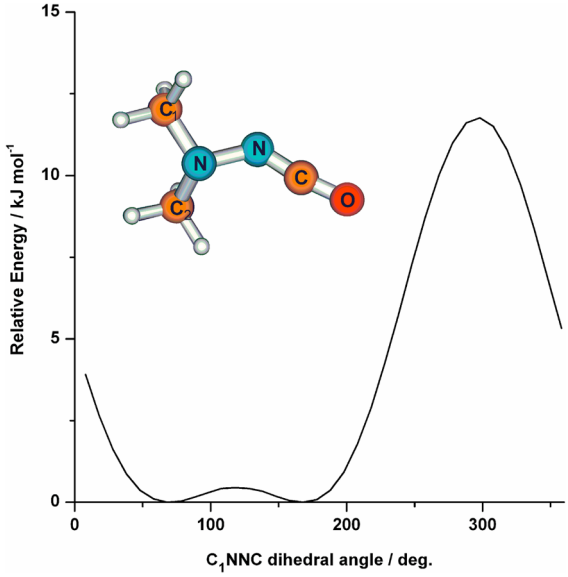

Figure 1. Structure of $(CH_3)_2N–NCO$ and its rotation around the N–N single bond, calculated at the B3LYP/aug-cc-pVTZ level.

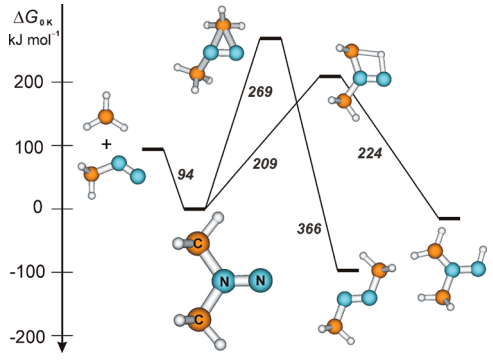

Figure 2. Structure of $(CH_3)_2N{=}N$ and its potential rearrangement to thermodynamically more stable isomers, calculated at the B3LYP/aug-cc-pVTZ level.

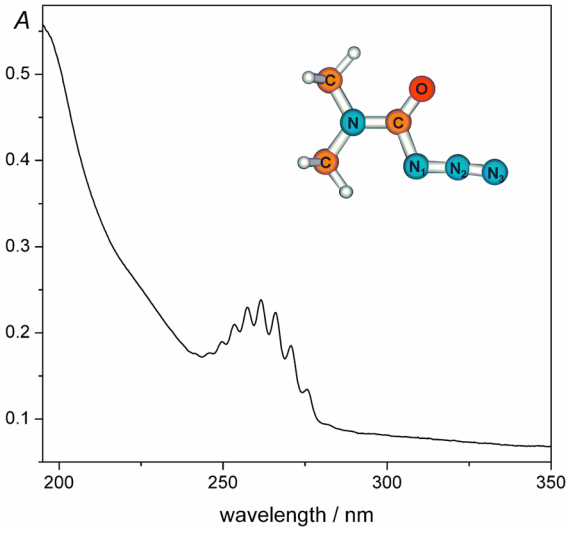

Figure 3. UV spectrum of the dimethylcarbamoyl azide precursor in an Ar matrix. The vibrational progression has a frequency of 675 cm^{-1}.

barrier for the retro-ene reaction to HOCN/HNCO and $CH_3N{=}CH_2$ (176 kJ mol^{-1}).[6] Both processes, elimination of

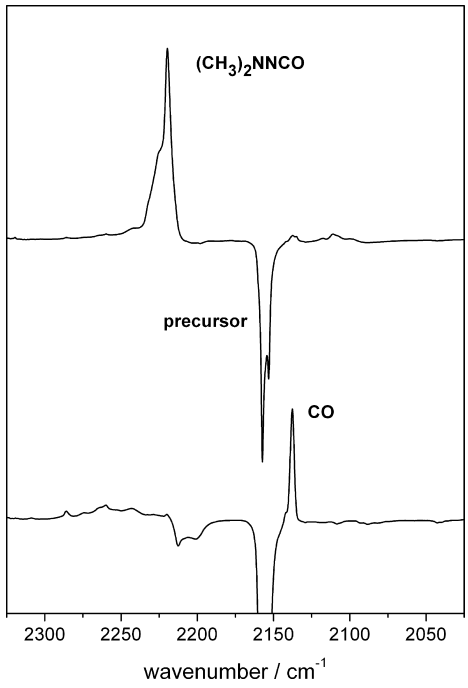

Figure 4. IR difference spectra (photolyzed minus deposited) recorded for dimethylcarbamoyl azide (precursor) after 5 (top) and 54 min (bottom) of BBUV irradiation using the xenon lamp. The ordinate gives the absorbance on an arbitrary scale.

HNCO and of CO, take place on FVT of $(CH_3)_2N–NCO$, itself generated by FVT of dimethylcarbamoyl azide .[6]

$(CH_3)_2N{=}N$ has a planar heavy-atom frame in its equilibrium structure with C_{2v} symmetry (Figure 2). The NN bond of the molecule is relatively short (1.203 Å), shorter than the typical N=N double bond in the isomeric *trans*-azomethane, *trans*-CH_3NNCH_3 (1.231 Å), but much longer than the triple bond in dinitrogen (1.091 Å). The double-bond character of the NN diazene bond is further confirmed by the calculated wavenumber of the NN stretch (1573 cm^{-1}), which is in the typical N=N stretching region. Potential isomerization of $(CH_3)_2N{=}N$ into the thermodynamically more stable *trans*-$CH_3N{=}NCH_3$ isomer or into the $CH_3N(CH_2)$-NH isomer, via methyl group and hydrogen atom migration, requires high activation energies ($\Delta G_{0\,K}$) of 269 and 209 kJ mol^{-1}, respectively. However, the calculated $CH_3–N$ bond dissociation energy is only 94 kJ mol^{-1} (Figure 2). As described below, this leads to decomposition of $(CH_3)_2N{=}N$ to ethane (by methyl radical recombination) and N_2.

Calculations predict that both molecules absorb in the near-UV region below about 350 nm (see Table S2 in the Supporting Information). Thus, photodecomposition of both $(CH_3)_2N–NCO$ and $(CH_3)_2N{=}N$ is expected during their generation by UV irradiation of an appropriate precursor below this wavelength.

Generation and Identification of $(CH_3)_2NNCO$ and $(CH_3)_2NN$. The UV spectrum of dimethylcarbamoyl azide in an Ar matrix is shown in Figure 3. The structured first absorption band is observed between 240 and 280 nm, and its photolysis was examined at 254 and 280 nm using the filtered radiation from a high-pressure mercury lamp and a xenon lamp, respectively. The 254 nm wavelength is close to the blue tail, and the 280 nm wavelength is at the red tail of the first absorption band. The decomposition of dimethylcarbamoyl

dx.doi.org/10.1021/jo402023m | J. Org. Chem. 2013, 78, 11985–11991

Table 1. Experimental and Calculated Wavenumbers ($\tilde{\nu}$, in cm^{-1}) and Infrared Intensities (I, in km mol^{-1}) for $(CH_3)_2N-NCO$

		calcd		
vibrational mode	TED[a]	$\tilde{\nu}$[b]	I[c]	exptl[d] (Ar matrix)
ν_1(a) CH str	CH(100)	2982 (3131)	15	3009
ν_2(a) CH str	CH(100)	2972 (3117)	16	n.o.
ν_3(a) CH str	CH(100)	2953 (3089)	21	2977
ν_4(a) CH str	CH(100)	2947 (3079)	15	n.o.
ν_5(a) CH str	CH(100)	2798 (2977)	95	n.o.
ν_6(a) CH str	CH(100)	2785 (2973)	33	n.o.
ν_7(a) NCO asym str	N=C(48), C=O(51)	2256 (2298)	1094	2226 (sh), 2220
ν_8(a) CH_3 asym def	HCH(16)(38)(33)	1463 (1512)	15	1474
ν_9(a) CH_3 asym def	HCN(88)	1417 (1495)	0.2	n.o.
ν_{10}(a) CH_3 asym def	HCN(88)	1448 (1491)	13	1451
ν_{11}(a) CH_3 asym def	HCN(89)	1434 (1478)	10	1440
ν_{12}(a) CH_3 sym def	HCN(91)	1444 (1465)	0.1	n.o.
ν_{13}(a) CH_3 sym def	HCN(99)	1406 (1438)	0.2	n.o.
ν_{14}(a) NCO sym str	NN(16), N=C(35), C=O(39)	1393(1420)	0.6	n.o.
ν_{15}(a) CH_3 rock	HCN(60), CN(14)	1213 (1246)	10	1217 ?
ν_{16}(a) CH_3 rock	HCN(41), CN(39)	1200 (1238)	3	n.o.
ν_{17}(a) CH_3 rock	HCN(80)	1150 (1181)	5	1166
ν_{18}(a) CH_3 rock	HCN(84)	1087 (1114)	3	1092
ν_{19}(a) CN asym str	CN(46), HCN(39)	1004 (1026)	13	1016, 1011
ν_{20}(a) CN sym str	CN(65), NN(18)	932 (962)	13	954, 952
ν_{21}(a) NN str	NN(42), NCO(24), CN(14)	735 (759)	19	755, 752
ν_{22}(a) NCO bend	NCO(53), NN(16), NNC(13)	633 (643)	30	623
ν_{23}(a) NCO bend	NCO(97)	545 (553)	20	n.o.
ν_{24}(a) CNN asym def	CNN(71)	452 (455)	9	n.o.
ν_{25}(a) def	CCNN(68), CNN(14)	390 (398)	13	n.o.
ν_{26}(a) CNN sym def	CNN(57), CCNN def(27)	381 (387)	2	n.o.
ν_{27}(a) CH_3 tors	HCNN(89)	232 (272)	0.4	n.o.
ν_{28}(a) CH_3 tors	HCNN(98)	229 (252)	0.2	n.o.
ν_{29}(a) NNC bend	NNC(82), NCO(12)	144 (147)	7	n.o.
ν_{30}(a) N–N tors	CNNC(100)	33 (36)	1	n.o.

[a]Total vibrational energy distribution (TED, in percent) from force field analysis based on B3LYP/aug-cc-pVTZ harmonic force constants. Contributions smaller than 10% are not listed. [b]Anharmonic wavenumbers (harmonic wavenumbers are given in parentheses), calculated at the B3LYP/aug-cc-pV(T+d)Z level. Isotopes: ^{12}C, ^{1}H, ^{14}N, ^{16}O. [c]Harmonic intensities, calculated at the B3LYP/aug-cc-pVTZ level. [d]Due to the presence of another molecule (N_2, CO) in the same site, the data presented might be slightly shifted in comparison to those of the free isolated molecule. Some of the bands are split due to site effects. n.o.= not observed.

azide and the formation of dimethylamino isocyanate (eq 1) was observed by IR spectroscopy at both of these wavelengths,

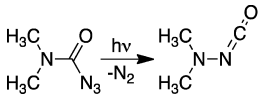

(1)

but the photolysis was very slow at 280 nm. Photolysis was also investigated using the unfiltered light of the mercury and xenon lamps (broad band UV irradiation, BBUV).

When the photolysis of dimethylcarbamoyl azide was monitored using UV spectroscopy, slow and fast disappearance of the characteristic UV band of the precursor was observed using 254 nm and BBUV irradiation, respectively. New UV bands, attributable to distinct photolysis products, were not detected, however, which indicates that photolysis products do not absorb in the near-UV region, or only weakly so due to low concentration and/or small oscillator strength.

IR difference spectra recorded during the BBUV photolysis of dimethylcarbamoyl azide using the xenon lamp are shown in Figure 4 and Figures S1–S9 of the Supporting Information. The most prominent product feature at the beginning of the photolysis is the IR band appearing at 2220 cm^{-1} with a shoulder at 2226 cm^{-1} (this is likely to be due to a combination band; the shoulder is always present, even when the isocyanate is generated by FVT of the azide) (Figure 4). The intensity of these bands first increased and then decreased and finally disappeared, indicating photodecomposition of the primary photolysis product. With a decrease in the intensity of this band, a characteristic IR band emerged at 2138 cm^{-1} and grew continuously during the photolysis. This band can be unambiguously assigned to carbon monoxide on the basis of its known IR spectrum and photostability. According to our calculations and previous experimental investigations (see above),[3,4] the IR bands at 2220/2226 cm^{-1} can be assigned to the antisymmetric stretch of the NCO moiety in dimethylamino isocyanate. All other bands which appear during the photolysis have much lower intensities. There are several low-intensity IR bands whose intensities increased and decreased together with the characteristic band at 2220 cm^{-1}, thereby indicating that they belong to the same species, namely dimethylamino isocyanate (see Table 1). The experimental spectrum recorded at the beginning of the photolysis and the calculated IR spectrum of dimethylamino isocyanate are shown in Figure 5. There is a good agreement between these spectra, especially when considering that some experimental bands will

dx.doi.org/10.1021/jo402023m | J. Org. Chem. 2013, 78, 11985–11991

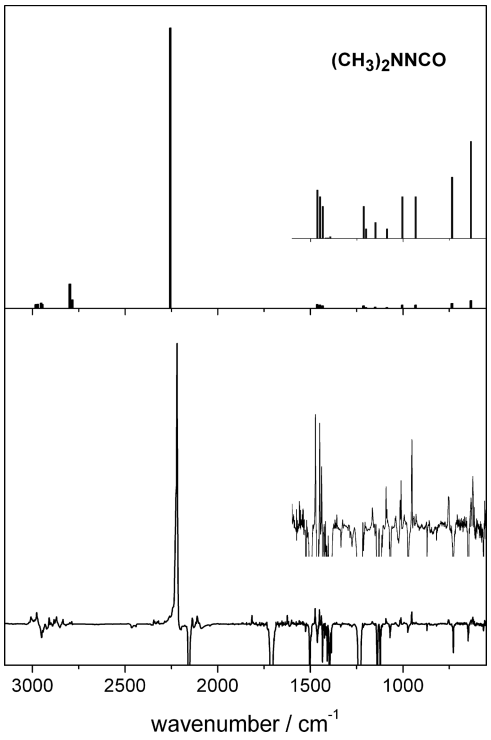

Figure 5. Computed IR spectrum of dimethylamino isocyanate (top) and IR difference (photolyzed − deposited) spectrum recorded after 5 min of BBUV irradiation of dimethylcarbamoyl azide using the xenon lamp (bottom). Insets are scaled by factors of 12 (top) and 7 (bottom). The ordinate gives the absorbance on an arbitrary scale.

Scheme 1. Photolysis of Dimethylcarbamoyl Azide, Dimethylamino Isocyanate, and 1,1-Dimethyldiazene

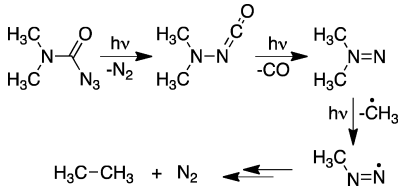

be obscured by the intense bands of the precursor. Intensity changes of all of these bands are shown in Figures S2−S8 in the Supporting Information.

After 54 min irradiation the IR bands of dimethylamino isocyanate were bleached, and characteristic bands of ethane emerged at 2991/2980, 2895, 1468, 1380/1375, and 829/820 cm^{-1} (see Figure S1 and Table S1, Supporting Information). The major final photolysis products are thus CO and ethane, which suggests that two nitrogen molecules must form from the precursor during consecutive decomposition steps (Scheme 1).

The photolysis was repeated using BBUV irradiation from a mercury lamp. Since these experiments produced essentially the same results as those using the xenon lamp with only minor alterations, these are not discussed in detail here (see Figures S10−S18, Supporting Information). We note that several low-intensity IR bands were detected during BBUV irradiation using either the xenon or the mercury lamp. The intensities of most of these bands first increased and then decreased during the photolysis, thereby indicating the decomposition of the corresponding species.

The photolysis of the dimethylcarbamoyl azide precursor was also investigated using narrow-band irradiation at 254 nm. The

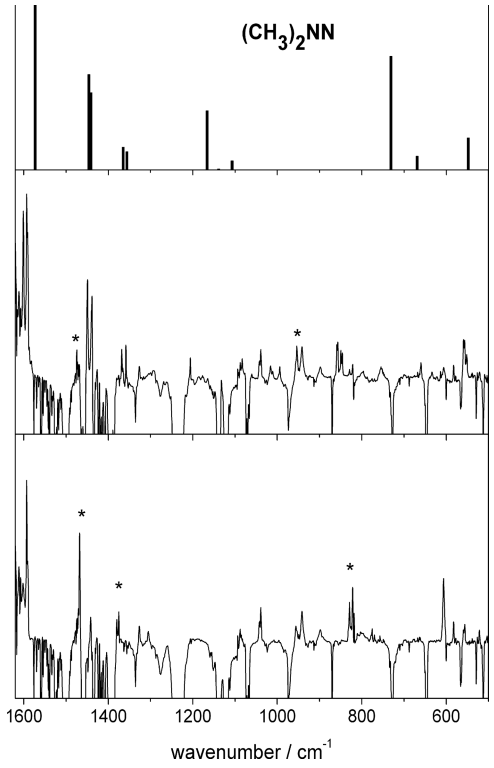

Figure 6. Computed IR spectrum of 1,1-dimethyldiazene (top) and difference (photolyzed − deposited) spectra recorded after 410 min photolysis at 254 nm (middle; the strongest IR bands of dimethylamino isocyanate are marked with an asterisk) and after consecutive 20 min BBUV irradiation (bottom; IR bands of ethane are marked with an asterisk) using the mercury lamp. The ordinate gives the absorbance on an arbitrary scale.

precursor decomposed slowly at this wavelength with the formation of dimethylamino isocyanate (see Figures S19−S25, Supporting Information). The isocyanate, however, decomposed at this wavelength with the formation of CO, similarly to the BBUV experiments. Parallel with the decomposition of dimethylamino isocyanate, new bands were observed at 1601, 1449, 1439, 1368, 1358, 1206, 660, and 552 cm^{-1}, whose intensity increased in concert on 254 nm photolysis, and they were all bleached upon consecutive BBUV irradiation (see Figure 6). These bands were also detected during the BBUV experiments, but with much lower intensities. According to the calculations (Table 2) and considering that the species decomposes with the formation of ethane upon BBUV irradiation (see Figure 6 and Figures S19−S25, Supporting Information), we assign these IR bands to 1,1-dimethyldiazene ($(CH_3)_2N{=}N$). The characteristic N=N stretching band was observed at 1601 cm^{-1}, which is in line with the corresponding N=N stretches of 1,1-diazene,[5] *N*-(2,2,6,6-tetramethylpiperidyl)nitrene,[7,8] and *N*-(2,2,5,5-tetramethylpyrrolidyl)-nitrene,[8] observed at 1574, 1595, and 1638 cm^{-1}, respectively. The photodecomposition route of dimethylamino isocyanate is thus very similar to the decomposition of the parent amino isocyanate, where the formation of 1,1-diazene and its decomposition to molecular nitrogen and hydrogen were detected.[4,5] All IR bands observed during the photodecomposition of dimethylcarbamoyl azide are given in Table 3. Assignment of all bands is not possible, as some may be due to combinations or overtones or to unassigned species formed during the photolysis. It is worth noting that the IR band at 607

dx.doi.org/10.1021/jo402023m | J. Org. Chem. 2013, 78, 11985−11991

Table 2. Experimental and Calculated Wavenumbers ($\tilde{\nu}$, in cm^{-1}) and Infrared Intensities (I, in km mol^{-1}) for $(CH_3)_2N{=}N$

vibrational mode	TED[a]	calcd $\tilde{\nu}$[b]	calcd I[c]	exptl[d] (Ar matrix)
$\nu_1(a_1)$ CH_3 asym str	CH(100)	3028 (3173)	3	n.o.
$\nu_{18}(b_2)$ CH_3 asym str	Ch(100)	3026 (3171)	2	n.o.
$\nu_{13}(b_1)$ CH_3 asym str	CH(100)	2972 (3113)	27	n.o.
$\nu_9(a_2)$ CH_3 asym str	CH(100)	2969 (3107)	0	n.o.
$\nu_2(a_1)$ CH_3 sym str	CH(100)	2939(3043)	23	n.o.
$\nu_{19}(b_2)$ CH_3 sym str	CH(100)	2938 (3034)	8	n.o.
$\nu_3(a_1)$ N=N str	NN (89)	1573 (1660)	37	1601
$\nu_{14}(b_1)$ CH_3 asym def	HCN(92)	1446 (1491)	21	1449
$\nu_4(a_1)$ CH_3 asym def	HCN(92)	1441 (1480)	17	1439
$\nu_{10}(a_2)$ CH_3 asym def	HCN(95)	1443 (1473)	0	n.o.
$\nu_{20}(b_2)$ CH_3 asym def	HCN(94)	1443 (1470)	5	n.o.
$\nu_5(a_1)$ CH_3 sym def	HCN(98)	1365 (1397)	5	1368
$\nu_{21}(b_2)$ CH_3 sym def	HCN(100)	1356 (1386)	4	1358
$\nu_{22}(b_2)$ CH_3 rock	HCN(52), CNN(24), CN(19)	1166 (1191)	13	1206
$\nu_6(a_1)$ CH_3 rock	HCN(76), CNC(10)	1139 (1155)	0.2	n.o.
$\nu_{15}(b_1)$ CH_3 rock	HCN(82), CCNN oop def (11)	1107 (1137)	2	n.o.
$\nu_{11}(a_2)$ CH_3 rock	HCN(95)	982 (1003)	0	n.o.
$\nu_{23}(b_2)$ CN asym str	CN(52), HCN(37), CNN(10)	731 (840)	25	n.o.[e]
$\nu_7(a_1)$ CN sym str	CN(99)	669 (713)	3	660
$\nu_{24}(b_2)$ CNN asym def	CNN(66), CN(30)	548 (558)	7	552
$\nu_{16}(b_1)$ oop def	CCNN oop. def (90)	447 (452)	0.1	n.o.
$\nu_8(a_1)$ CNN sym def	CNN(88)	412 (412)	2	n.o.
$\nu_{17}(b_1)$ CH_3 tors	HCNN(100)	168 (169)	1	n.o.
$\nu_{12}(a_2)$ CH_3 tors	HCNN(100)	153 (97)	0	n.o.

[a]Total vibrational energy distribution (TED, in percent) from force field analysis based on B3LYP/aug-cc-pVTZ harmonic force constants. Contributions smaller than 10% are not listed. [b]Anharmonic wavenumbers (harmonic wavenumbers are in parentheses), calculated at the B3LYP/aug-cc-pV(T+d)Z level. Isotopes: ^{12}C, ^{1}H, ^{14}N. [c]Harmonic intensities, calculated at the B3LYP/aug-cc-pVTZ level. [d]Due to the presence of other molecules (N_2, CO) in the same site, the data presented might be slightly shifted in comparison to those of the free isolated molecule. Some of the bands are split due to site effects. n.o.= not observed. [e]Overlapping with strong azide band.

cm^{-1} most likely belongs to the CH_3 radical (see Figure S25, Supporting Information). This characteristic, strongest IR band of the methyl radical was detected earlier at 603 and 611 cm^{-1} in argon and nitrogen matrices,[9] respectively. Thus, it can be

Table 3. Experimentally Observed Vibrational Absorptions (cm^{-1}) Formed during the Photolysis of Dimethylcarbamoyl Azide[a]

3009	$(CH_3)_2NNCO$	1217?	$(CH_3)_2NNCO$
2991, 2980	ethane	1206	$(CH_3)_2NN$
2977	$(CH_3)_2NNCO$	1166	$(CH_3)_2NNCO$
2910	$(CH_3)_2NNCO$?	1094	?
2895, 2891	ethane	1092	$(CH_3)_2NNCO$
2870	$(CH_3)_2NNCO$?	1087	?
2835	?	1042, 1039	?
2261	HNCO[b]	1060	?
2226 (sh), 2220	$(CH_3)_2NNCO$	1016, 1011	$(CH_3)_2NNCO$
2138	CO	994	?
1815	?	954, 952	$(CH_3)_2NNCO$
1624	water impurity	942	?
1601	$(CH_3)_2NN$	930	?
1593, 1591	?	898	?
1587, 1582	?	859, 857	?
1474	(CH3)2NNCO	850, 846	?
1468	ethane	829, 820	ethane
1451	$(CH_3)_2NNCO$	755, 752	$(CH_3)_2NNCO$
1449	$(CH_3)_2NN$	660	$(CH_3)_2NN$
1440	$(CH_3)_2NNCO$	633	?
1439	$(CH_3)_2NN$	623	$(CH_3)_2NNCO$
1380, 1375	ethane	607	CH_3 radical[b]
1368	$(CH_3)_2NN$	583	?
1358	$(CH_3)_2NN$	559, 557	?
1327	?	552	$(CH_3)_2NN$
1305	?		

[a]For relative intensities see Figures 3–6 and Figures S1–S25 (Supporting Information). [b]See text.

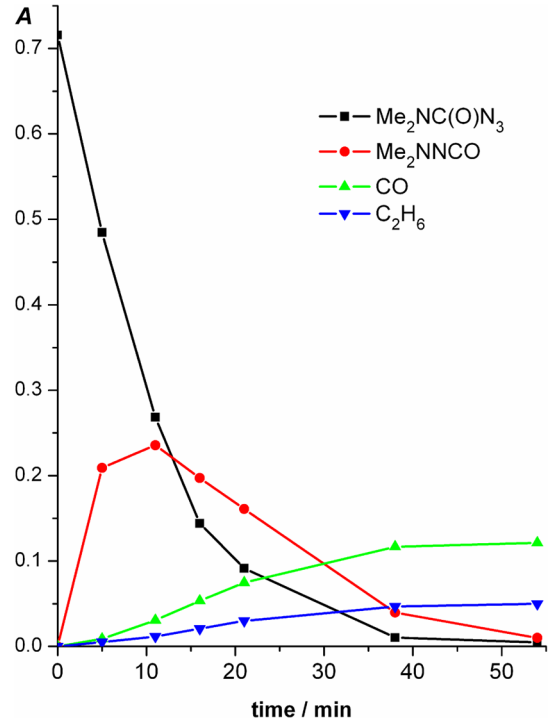

Figure 7. Intensity changes (A, absorbance) of IR bands at 2157 ($Me_2NC(O)N_3$ precursor), 2220 (Me_2NNCO), 2138 (CO), and 2991 cm^{-1} (ethane) during BBUV irradiation using the xenon lamp. Note that the intensities are not weighted according to extinction coefficients.

dx.doi.org/10.1021/jo402023m | J. Org. Chem. 2013, 78, 11985–11991

assumed that ethane is formed by the recombination of methyl radicals eliminated from the diazene. The main photodecomposition route of dimethylcarbamoyl azide is summarized in Scheme 1, and the temporal evolution of each species is illustrated in Figure 7.

We now turn to the supposed formation of HNCO and CH_3NC on photolysis of dimethylcarbamoyl azide in a neon matrix at 6 K as reported by Lwowski and Wilde et al.[3] An IR band observed at 2141 ± 2 (s) cm^{-1} was ascribed to CH_3NC. Because the known absorption of CH_3NC is at 2166 cm^{-1}, it was assumed that CH_3NC was complexed with HNCO in the neon matrix. However, our results reported above indicate that CH_3NC should not form. In fact, CO in Ne absorbs at 2141.2 cm^{-1}.[10] Therefore, we conclude that the compound assumed to be CH_3NC was in fact CO.

The formation of HNCO (2260 ± 2 (m-s) cm^{-1}) reported by Lwowski and Wilde is probably correct, although very little HNCO is formed in our photolyses (see the very minor band at 2261 cm^{-1} in Figure 4 and in Table 3). However, on FVT of dimethylcarbamoyl azide at 500−600 °C, both dimethylamino isocyanate (2218 cm^{-1}) and HNCO (2260 cm^{-1}) are formed, the latter via a retro-ene type reaction of the isocyanate.[6] CO (2138 cm^{-1}) is also formed on FVT and is very prominent already at 500 °C. Rigorous examination of authentic matrices containing CH_3NC ascertained that this compound is definitely not formed. Thus, dimethylcarbamoyl azide appears to undergo the same principal reactions (Scheme 1) on photolysis and on thermolysis.

CONCLUSION

The photodecomposition of dimethylcarbamoyl azide in a cryogenic argon matrix yields dimethylamino isocyanate (2220, 2226 cm^{-1}), 1,1-dimethyldiazene (1601, 1445, 1439 cm^{-1}), and ethane by sequential elimination of N_2, CO, and N_2 as determined by matrix isolation IR spectroscopy. Ethane formation is ascribed to recombination of methyl radicals (observed at 607 cm^{-1}). The main decomposition channel is shown in Scheme 1. Dimethylamino isocyanate and 1,1-dimethyldiazene were structurally characterized by quantum-chemical methods. Both molecules have singlet electronic ground states. $(CH_3)_2N-N=C=O$ has a trans-bent NNCO frame with C_1 molecular symmetry. $(CH_3)_2N=N$ has a planar heavy-atom frame with C_{2v} symmetry and a short NN double bond.

EXPERIMENTAL AND COMPUTATIONAL METHODS

Dimethylcarbamoyl azide was synthesized from dimethylcarbamoyl chloride and sodium azide according to a literature method[11] and purified by column chromatography (silica gel, dichloromethane). The purity of the azide was checked by NMR and IR measurements. ^1H NMR ($CDCl_3$, 302 K): 2.85 and 2.89 ppm. ^{13}C NMR ($CDCl_3$, 302 K): 36.5, 37.1, and 156.8 ppm. The ATR-IR spectrum is provided in Figure S26 (Supporting Information). The precursor for the azide, dimethylcarbamoyl chloride, was synthesized according to a published method,[12] and all other starting materials were commercial products.

For matrix isolation experiments, the vapor of the degassed precursor was premixed with argon (from Messer, purity 99.9997%) in a 1:1000 mole ratio in a glass vacuum line. The gas mixtures were deposited onto a 10 K CsI window for IR and onto a 12 K quartz window for UV spectroscopic measurements. The flow rates were about 1.2 and 0.3 cm^3 min^{-1} for IR and UV measurements, respectively. The CsI and quartz windows were mounted on a cold head cooled by a CTI Cryogenics closed-cycle refrigerator. The temperature of the cold head was controlled by a thermostat equipped with a silicon diode thermometer. A 125 W high-pressure mercury lamp and a xenon lamp were used as photolysis sources. The deposited matrix was irradiated through a quartz window and an interference filter (254 nm filter for the Hg lamp and 280 nm filter for the Xe lamp). The interference filters had a full width at half-height of 10 and 25 nm at 254 and 280 nm, respectively. For broad-band UV photolysis (BBUV) the mercury or the xenon lamps were used without any filter.

Infrared spectra were recorded on a spectrometer equipped with a KBr beam splitter and a DTGS detector. A total of 250−1000 scans were accumulated at 1 cm^{-1} resolution in the 400−4000 cm^{-1} spectral window. A Happ-Genzel apodization function, a Metz phase correction using phase resolution of 32 cm^{-1}, and a zero filling factor of 4 were applied.

Absorption UV spectra were recorded with a 5 nm min^{-1} scan rate, 0.333 nm step size, and 1 nm spectral bandwidth. Data were collected in the 190−350 nm spectral region.

Quantum-chemical calculations were performed using the GAUSSIAN09 program package.[13] Equilibrium geometries and harmonic vibrational frequencies were calculated using the B3LYP[14] method and the aug-cc-pVTZ basis set.[15] Anharmonic vibrational corrections, within the framework of second-order vibrational perturbation theory,[16] were obtained at the same level. Singlet excitation energies and oscillator strengths were calculated applying the TD-B3LYP[17] and SAC-CI[18] methods, using the B3LYP equilibrium geometries.

For characterization of the normal vibrational modes of $(CH_3)_2NNCO$ and $(CH_3)_2NN$, the total vibrational energy distribution (TED), which provides a measure of the internal coordinate contributions,[19] was determined using Program Scale 3.[20]

ASSOCIATED CONTENT

Supporting Information

Figures and tables giving the calculated equilibrium geometries, excitation energies, vibrational wavenumbers and IR intensities of investigated molecules, enlarged IR spectra of photolysis products, detected IR bands, and the IR spectrum of the precursor. This material is available free of charge via the Internet at http://pubs.acs.org.

AUTHOR INFORMATION

Corresponding Authors

*E-mail for T.P.: pasinszki@chem.elte.hu.
*E-mail for C.W.: wentrup@uq.edu.au.

Notes

The authors declare no competing financial interest.

ACKNOWLEDGMENTS

We thank the Hungarian Scientific Research Fund for financial support of the project (Grant Nos. OTKA K101164 and K75877).

REFERENCES

(1) Wentrup, C.; Finnerty, J. J.; Koch, R. *Curr. Org. Chem.* **2011**, *15*, 1745−1759.
(2) (a) Gibson, H. H., Jr.; Weissinger, K.; Abashawl, A.; Hall, G.; Lawshae, T.; LeBlanc, K.; Moody, J. *J. Org. Chem.* **1986**, *51*, 3858−3861. (b) Lwowski, W.; Kanemasa, S.; Murray, R. A.; Ramakrishnan, V. T.; Thiruvengadam, T. K.; Yoshida, K.; Subbaraj, A. *J. Org. Chem.* **1986**, *51*, 1719−1723.
(3) Lwowski, W.; de Mauriac, R. A.; Thompson, M.; Wilde, R. E.; Chen, S.-Y. *J. Org. Chem.* **1975**, *40*, 2608−2612.
(4) Teles, J. H.; Maier, G. *Chem. Ber.* **1989**, *122*, 745−748.
(5) (a) Sylwester, A. P.; Dervan, P. B. *J. Am. Chem. Soc.* **1984**, *106*, 4648−4650. (b) Teles, J. H.; Maier, G.; Hess, B. A., Jr.; Schaad, L. J. *Chem. Ber.* **1989**, *122*, 749−752.

(6) Koch, R.; Finnerty, J. J.; Murali, S.; Wentrup, C. *J. Org. Chem.* **2012**, *77*, 1749−1759.
(7) Hinsberg, W. D., III; Dervan, P. B. *J. Am. Chem. Soc.* **1978**, *100*, 1608−1610.
(8) Hinsberg, W. D., III; Schultz, P. G.; Dervan, P. B. *J. Am. Chem. Soc.* **1982**, *104*, 766−773.
(9) Milligan, D. E.; Jacox, M. E. *J. Chem. Phys.* **1967**, *47*, 5146−5156.
(10) Pirim, C.; Krim, L. *Phys. Chem. Chem. Phys.* **2011**, *13*, 19454−19459.
(11) Allan, E. A.; Hobson, R. F.; Reeves, L. W.; Shaw, K. N. *J. Am. Chem. Soc.* **1972**, *94*, 6604−6611.
(12) Schindler, N.; Plöger, W. *Chem. Ber.* **1971**, *104*, 969−971.
(13) Frisch, M. J. et al. *GAUSSIAN 09 (Revision B.01)*, Gaussian, Inc., Wallingford, CT, 2009 (the full reference is available in the Supporting Information).
(14) (a) Becke, A. D. *J. Chem. Phys.* **1993**, *98*, 5648−5652. (b) Lee, C.; Yang, W.; Parr, R. G. *Phys. Rev. B* **1988**, *37*, 785−789.
(15) (a) Dunning, T. H., Jr. *J. Chem. Phys.* **1989**, *90*, 1007−1023. (b) Kendall, R. A.; Dunning, T. H., Jr.; Harrison, R. J. *J. Chem. Phys.* **1992**, *96*, 6796−6806. (c) Woon, D. E.; Dunning, T. H., Jr. *J. Chem. Phys.* **1993**, *98*, 1358−1371.
(16) (a) Nielsen, H. H. *Rev. Mod. Phys.* **1951**, *23*, 90−136. (b) Allen, W. D.; Yamaguchi, Y.; Császár, A. G.; Clabo, D. A., Jr.; Remington, R. B.; Schaefer, H. F., III *Chem. Phys.* **1990**, *145*, 427−466.
(17) Scalmani, G.; Frisch, M. J.; Mennucci, B.; Tomasi, J.; Cammi, R.; Barone, V. *J. Chem. Phys.* **2006**, *124*, 094107 and references cited therein.
(18) Toyota, K.; Mayumi, I.; Ehara, M.; Frisch, M. J.; Nakatsuji, H. *Chem. Phys. Lett.* **2003**, *367*, 730−736 and references cited therein.
(19) Keresztury, G.; Jalsovszky, G. *J. Mol. Struct.* **1971**, *10*, 304−305.
(20) Pongor, G. *Program Scale 3*; Department of Theoretical Chemistry, Eötvös Loránd University, Budapest, Hungary, 1993.